APPLIED ORGANOMETALLIC CHEMISTRY, VOL. 12, 173–187 (1998)

Evaluation of the simultaneous use of Cp_2VMe_2 and $CpTiCl_2N(SiMe_3)_2$ as precursors to ceramic thin films containing titanium and vanadium: Towards titanium–vanadium carbonitride

L. Valade,* C. Danjoy, B. Chansou, E. Rivière, J.-L. Pellegatta, R. Choukroun and P. Cassoux

Equipe Précurseurs Moléculaires et Matériaux, Laboratoire de Chimie de Coordination, CNRS, 205 route de Narbonne, 31077 Toulouse Cedex, France

Ceramic thin films containing titanium, vanadium, carbon, oxygen and nitrogen were obtained on steel substrates at 873 K, under nitrogen and helium gases and at low pressure, by chemical vapor deposition (CVD) from two organometallic precursors, $CpTiCl_2N(SiMe_3)_2$ and Cp_2VMe_2 (Cp, cyclopentadienyl). Independent TG–DTA–MS and CVD studies of the two precursors showed their ability to co-decompose within compatible temperature and pressure domains. The mechanism of the reactions occurring inside the CVD apparatus was also approached by GC–MS and NMR analyses of the condensed decomposition products. CVD conducted under He gas confirmed that the formation of nitride resulted from the nitrogen atoms of the precursor, but the nitrogen content in the films remained lower than approx. 5%. Higher nitrogen contents (up to 12%) were only obtained when using ammonia as a carrier gas. Both precursors being air- and moisture-sensitive, high-purity CVD equipment was used to reduce oxycarbide formation. © **1998 John Wiley & Sons, Ltd.**

Appl. Organometal. Chem. **12**, 173–187 (1998)

Keywords: Metal-organic chemical vapor deposition (MOCVD); precursors; titanium; vanadium; carbonitride

Received 10 December 1996; accepted 14 April 1997

*Correspondence to: L. Valade, Equipe Précurseurs Moléculaires et Matériaux, Laboratoire de Chimie de Coordination, CNRS, 205 route de Narbonne, 31077 Toulouse Cedex, France.

1 INTRODUCTION

The need for alternative low-energy processes in materials production has led to the '*Chimie douce*' concept,[1] involving the use of molecular precursors from which materials could be prepared at much lower temperature than those for conventional solid-state chemistry methods. Thus, Sol–gel and metal-organic chemical vapor deposition (MOCVD) techniques have gained increasing interest for the preparation of thin films of metals, semiconductors and ceramics (see, for example, Refs 2–4).

In the case of the preparation of ceramic thin films, molecular precursors are often selected on the basis of predicted mechanisms; in some cases, these may be inferred from thermal decomposition analyses, checked by chemical analysis of the decomposition products evolving during the CVD process, and finally confirmed by characterization of the expected films.[5]

We have been interested in the design and study of 'single-source' precursors to titanium and vanadium carbide and nitride ceramic thin films.[6] For example, vanadocene[7] and $(C_5H_4CMe_3)_2V$[8] have been used in the chemical vapor deposition of vanadium carbide, and $V(NEt_2)_4$[9] and $Cl_3VN(t\text{-}Bu)$[10] for the preparation of vanadium carbonitride. Likewise, Hoffmann and co-workers have shown that titanium and vanadium nitrides may be obtained from $Ti(NMe_2)_4$ and $V(NMe_2)_4$[11,12] in the presence of ammonia, and Winter *et al.* successfully used $TiCl_4(NH_3)_2$ to prepare titanium nitride films.[13] Titanium and vanadium carbide and nitride are known to exhibit outstanding thermal, mechanical, chemical and conductive properties, as encountered in many ceramic materials.[14,15] Their good abrasion resistance and low friction also make

 CCC 0268–2605/98/030173–15 $17.50

them attractive for protective-coating applications.[16–18] Moreover, as they crystallize in the same face-centered cubic (fcc) system with closely similar parameters, they can form solid solutions over a wide range of compositions.[19] Such titanium–vanadium carbonitride ceramics could possibly exhibit improved hardness compared with those of the corresponding binary phases, and they could be used for protective coating of steel. With this in mind, we have extended our previous studies to the preparation of ceramic thin films of titanium–vanadium carbonitride by simultaneously using two precursors containing titanium and vanadium, respectively. Among the numerous possible precursor candidates,[6–13, 20–25] we have selected $CpTiCl_2N(SiMe_3)_2$ and Cp_2VMe_2 (Cp, cyclopentadienyl). We report here on the thermoanalytical, mass-spectrometry and CVD studies of each of these compounds. We will also describe the co-decomposition of both of these compounds using a 'two-precursor' CVD process for the preparation of ceramic thin films containing titanium *and* vanadium, carbon, nitrogen and oxygen.

2 RESULTS AND DISCUSSION

2.1 $CpTiCl_2N(SiMe_3)_2$

In a previous paper, we have described[22] the synthesis of $CpTiCl_2N(SiMe_3)_2$, its thermoanalytical study (dynamic mode) and the CVD preparation of TiCN thin films at 873 K using this precursor molecule. Coupled MS analysis of TG (thermo-gravimetry) decomposition products indicated the formation of Me_3SiCl and CpH as the major components, and small amounts of $(Me_3Si)_2NH$ corresponding to Ti–N bond cleavage. The small nitrogen content of the films obtained under CVD conditions (873 K) was attributed to this Ti–N bond cleavage, and the deposition of excess carbon was attributed to the decomposition of the Cp groups.[22]

A further evaluation of the utility of $CpTiCl_2N(SiMe_3)_2$ as one of the two precursors needed for the MOCVD preparation of quaternary TiVCN thin films was obtained from additional MS studies and TG–DTA–MS (thermo-gravimetry/differential thermal analysis /mass Spectrometry) analyses in isothermal mode, and by varying the CVD conditions (temperature, pressure, carrier gas).

The mass spectrum of the $CpTiCl_2N(SiMe_3)_2$ molecule (Fig. 1) showed the parent peak (m/z = 343) with an isotopic pattern identical to the calculated one. The major fragmentation peaks have been assigned as shown in Scheme 1, after simulation of the isotopic distribution for each proposed formula. The observation of $Me_3SiNHSiMe_2^+$ (m/z = 146) and $CpTi^{+\cdot}$ (m/z = 113) fragments confirms Ti–N bond cleavage. Cl- and Si-containing fragments were also observed in the mass

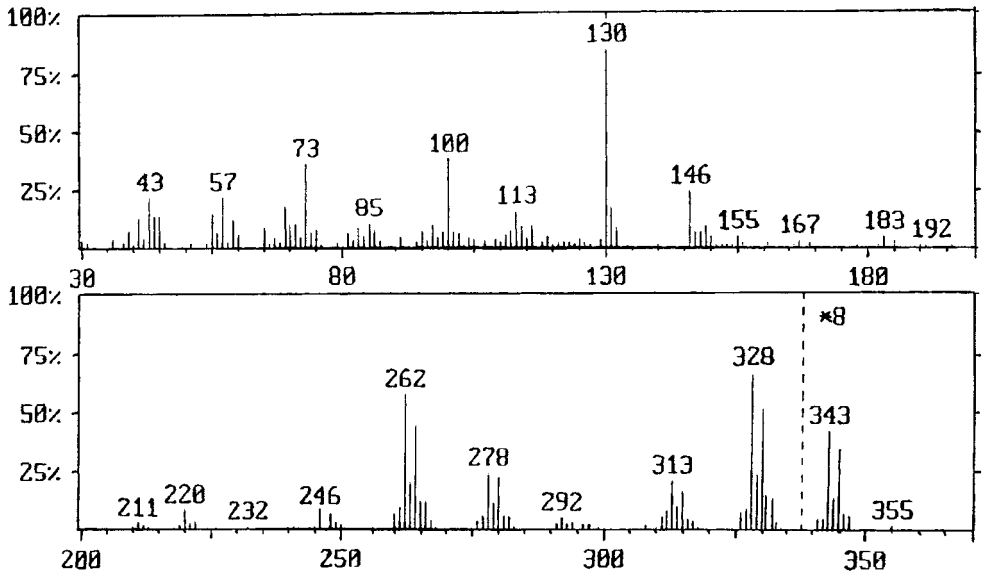

Figure 1 EI mass spectrum of $CpTiCl_2N(SiMe_3)_2$.

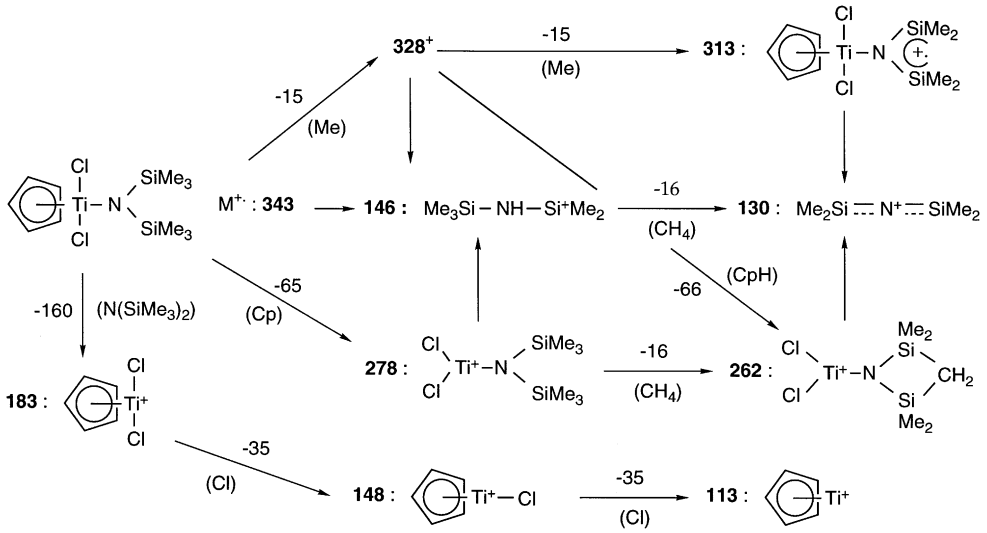

Scheme 1

spectra. The MS fragmentation pattern may give a qualitative indication of the relative strength of the bonds which may be used for predicting the thermal behavior of a molecule-based precursor. However, the energies involved in both processes (a few electronvolts for thermal decomposition, i.e. 10^3-fold weaker than for ionisation) are very different, so that molecular fragmentation under electron impact may not resemble in all cases the radical pathways of thermal decomposition. It should be noted, however, that in the present case the results of MS analysis of $CpTiCl_2N(SiMe_3)_2$ seem consistent with the TG–MS data.

In order to examine the nature of the gas phase transported in the CVD reactor, $CpTiCl_2N(SiMe_3)_2$ samples were heated under nitrogen at constant temperature and their weight losses were recorded as a function of time (isothermal mode; Fig. 2). At 393 K, the weight loss varied slowly with time and the constant vaporization rate confirmed a zero-order kinetic process consistent with the pure sublimation of the compound. At 493 K, the formation of a residue indicated the decomposition of the molecule. Simultaneous MS analysis of the gas phase showed the formation of Me_3SiCl and CpH as major components. Ti–N bond cleavage occurred, but only small amounts of resulting $(Me_3Si)_2NH$ were found. TG–DTA–MS analysis under helium showed identical results.

CVD experiments were run using the CVD unit equipped with a primary pump and by varying the gas flow rate (3 and 7 l h^{-1}), the substrate temperature (from 623 to 873 K) and the pressure (5 and 20 Torr). Deposits were obtained on silicon and steel substrates and analyzed by SEM–EDS (scanning electron microscopy–energy dispersive spectroscopy) and XPS (x-ray photo-electron spectroscopy) (Table 1). All deposits contained titanium, carbon, nitrogen and oxygen. (Oxygen contamination of these films probably results from an imperfect purification of the CVD unit which is only equipped with a primary pumping system. The oxygen content can be considerably reduced by

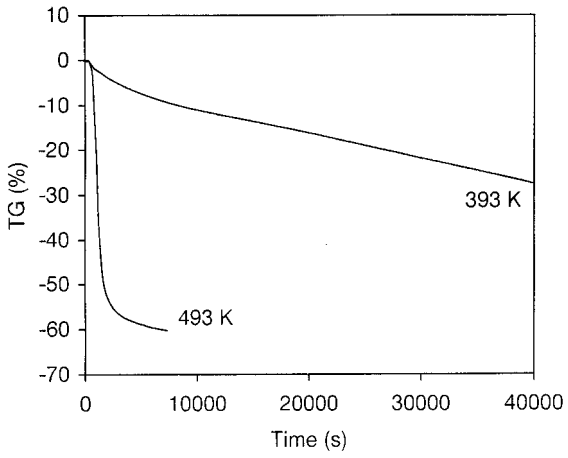

Figure 2 Thermogram of $CpTiCl_2N(SiMe_3)_2$ showing the percentage weight loss as a function of time for two temperature levels. N_2 carrier gas (1 l h^{-1}).

Table 1 Selected CVD conditions for $CpTiCl_2N(SiMe_3)_2$ and corresponding analysis of the deposits

Mass of precursor (mg)	Pressure (Torr)	Nitrogen flow rate ($l\ h^{-1}$)	Substrate temperature (K)	Substrate type	Deposit composition from XPS[a] (at%)					
					Ti	C	N	O	Si	Cl
365	5 and 20	7	623	Si, steel	28	23	7	40	1	1
380	5	7	773	Si, steel	22	25	5	47	5	—
600	20	3	873	Si	22	18	1	50	8	0.5

[a] Semi-quantitative results.

using a CVD unit equipped with a high-vacuum diffusion pump, as will be shown in Section 2.6). XPS showed that the titanium was present as carbide, nitride and oxide. Carbon appeared as carbide and graphite, at all temperatures. Silicon and chlorine contamination was low (close to the detection limit) at low temperature (623 K). The fortunately low chlorine content is important in evaluating the feasibility of this precursor, as it is known that residual Cl affects the crystallinity, microhardness and adhesion strength of titanium carbonitride.[26] At 873 K, a significant increase in the silicon content was accompanied by a decrease in the nitrogen content. The variation of the pressure and gas flow rate influenced the thickness of the deposits essentially: an increase in the pressure (to 20 Torr) and a decrease in the gas flow rate (to $3\ l\ h^{-1}$) resulted in the formation of thicker deposits.

2.2 Cp_2VMe_2

The MS spectrum of $Cp_2\ VMe_2$ is shown on Fig. 3. The fragmentation peaks have been assigned following Scheme 2. The fragmentation is initiated by the loss of the two methyl groups. The pattern obtained at lower masses corresponds to that of Cp_2V.[27] The peak at $m/z = 80$ may be assigned to the formation of CpMe and the one at $m/z = 130$ to the occurrence of $CpV{=}CH_2$ species.

The thermoanalytical study of Cp_2VMe_2 was run in the dynamic mode under nitrogen and helium

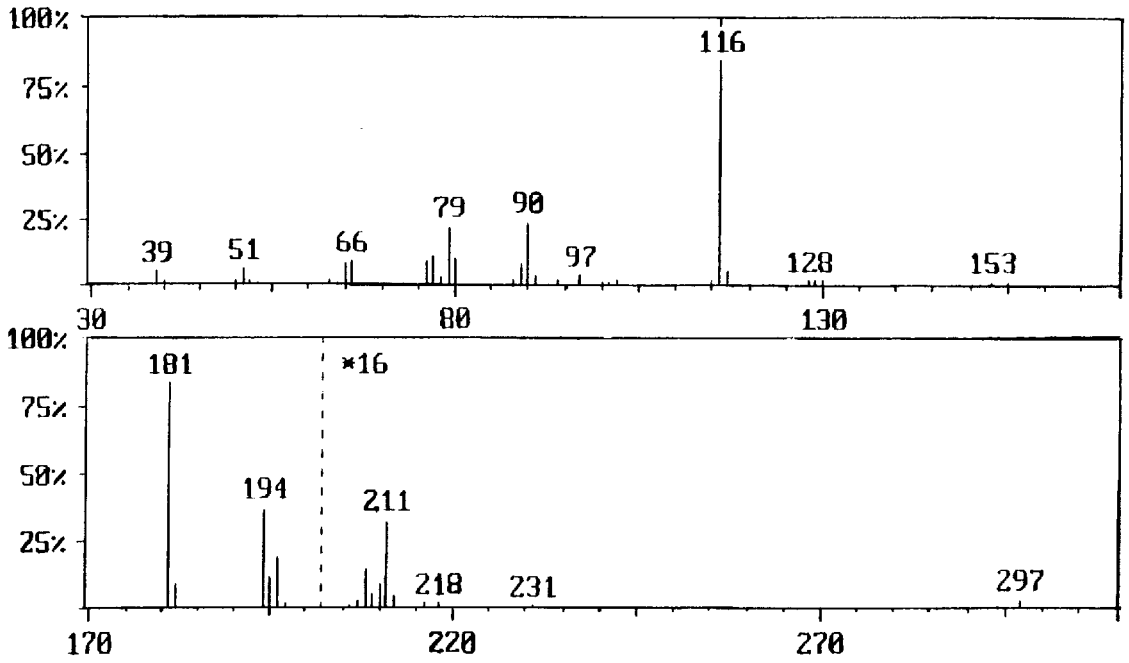

Figure 3 EI mass spectrum of Cp_2VMe_2.

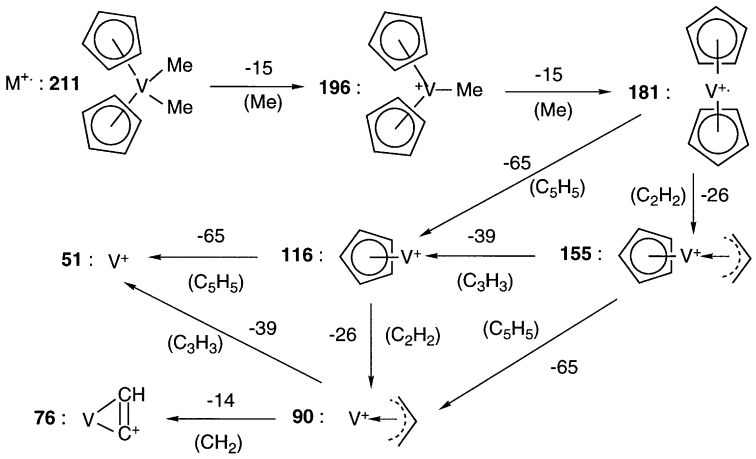

Scheme 2

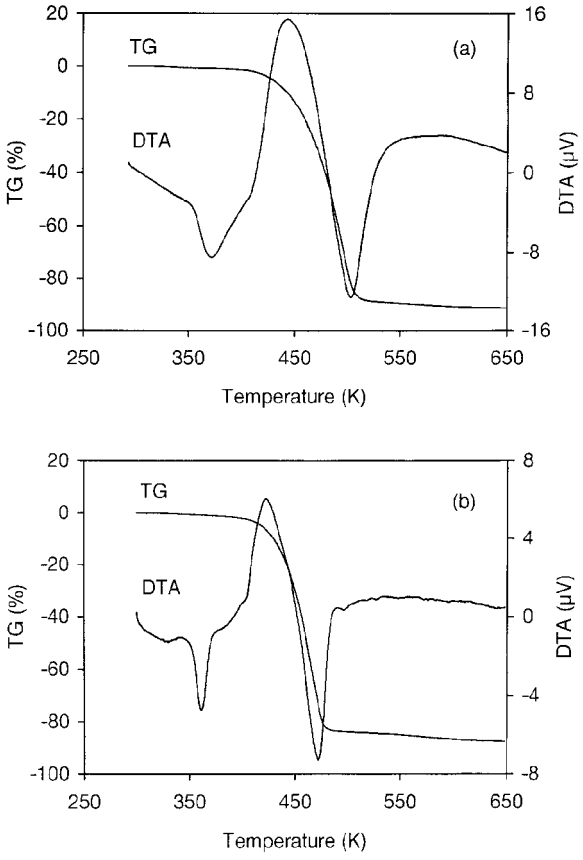

Figure 4 Thermogram of Cp_2VMe_2 showing the percentage weight loss (left) and the DTA signals (right). (a) N_2 carrier gas (1 l h^{-1}) and 10 K min^{-1} temperature ramp. (b) He carrier gas (1 l h^{-1}) and 10 K min^{-1} temperature ramp.

(Fig. 4). With both gases, the weight loss occurred in one major step (weight loss 88%/N_2 and 83%/He) followed by a smaller one (*ca* 4% with both gases). The decomposition temperature domain is narrower under helium than under nitrogen. The DTA curves exhibit three thermal events: melting at 353 K, exothermic reaction at 413 K/N_2 and 403 K/He, and endothermic reaction at 433 K/N_2 and 423 K/He. Simultaneous MS analysis of the decomposition gases was run at atmospheric pressure under nitrogen. Of particular interest was the detection of CpMe ($m/z = 80$) and $C_5H_4Me_2$ ($m/z = 94$) species as major components of the gas phase. This result is consistent with pyrolysis studies of other Cp_2MMe_2 compounds (M = Ti, Zr), where substituted cyclopentadienyl species resulting from the migration of the methyl groups to the Cp rings have been observed.[28,29] Methane ($m/z = 16$) and CpH ($m/z = 66$) were also detected, along with C_3H_3 ($m/z = 39$) produced by the fragmentation of the Cp group. The variation of the peak intensities with temperature for the main detected species is reported in Fig. 5. The exothermic peak obviously corresponded to the formation of methane and CpMe species. The low-temperature endothermic peak was attributed to both melting (the reversibility of the DTA peak was checked; Fig. 6 and decomposition of the molecule (CpH was detected at this same temperature). At higher temperatures, loss of CpH continued in two stages: the first corresponded to the high-temperature decomposition, endothermic peak and the second to the last 4% weight loss in the TG curve. Under helium the decomposition process of

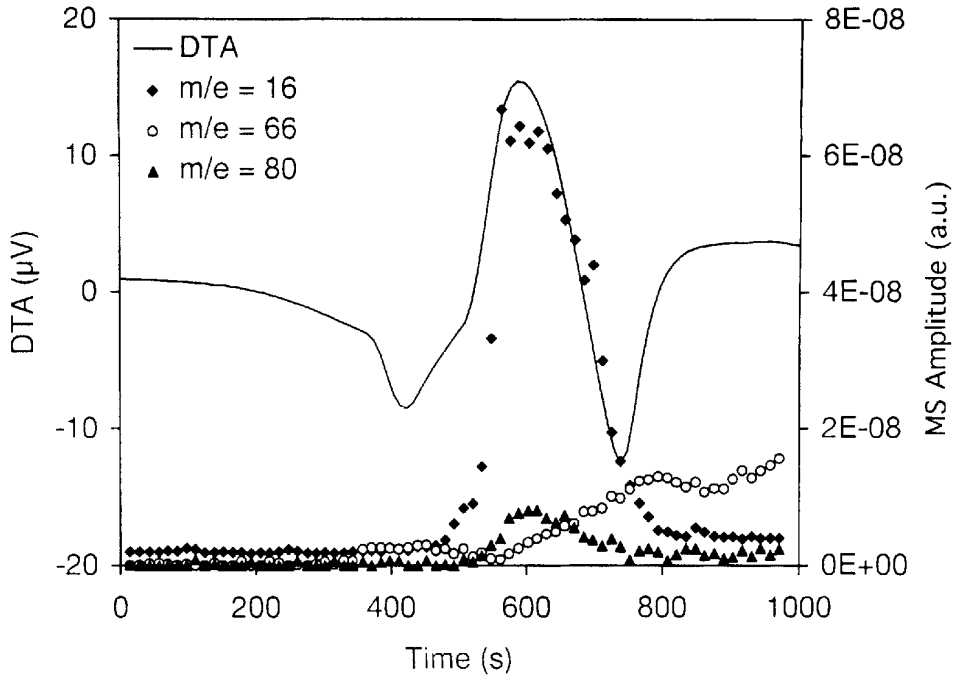

Figure 5 Thermogram of Cp_2VMe_2 showing the DTA signals (left) and the abundance of MS detected species (right). N_2 carrier gas ($1\,l\,h^{-1}$) and $20\,K\,min^{-1}$ temperature ramp.

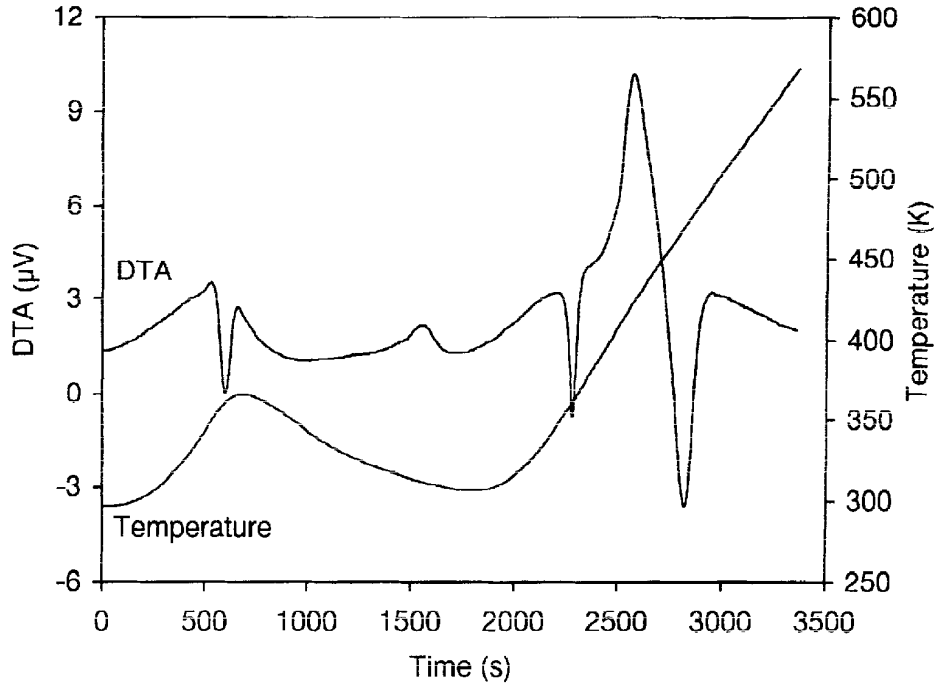

Figure 6 Thermogram of Cp_2VMe_2 showing the reversibility of the DTA melting peak (left) and the temperature program (right). He carrier gas ($1\,l\,h^{-1}$).

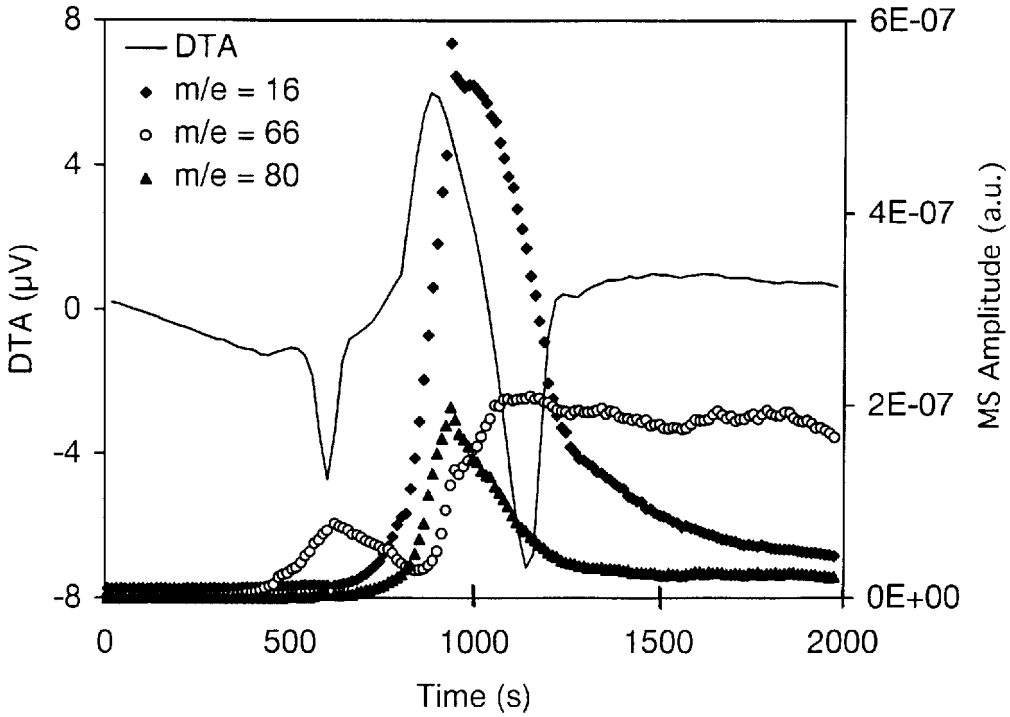

Figure 7 Thermogram of Cp_2VMe_2 showing the DTA signals (left) and the abundance of MS detected species (right). He carrier gas ($1\,l\,h^{-1}$) and $10\,K\,min^{-1}$ temperature ramp.

Cp_2VMe_2 was similar to that observed under nitrogen and the same products were detected in the gas phase: thermally activated rearrangement reactions occurred, and led to the formation of CpMe and $C_5H_4Me_2$ (Fig. 7).

CVD experiments have been conducted, using the CVD unit equipped with a primary pump, under nitrogen (3 and $7\,l\,h^{-1}$), and by varying the substrate temperature (573–873 K) and the pressure (2–5 Torr). Selected CVD conditions are gathered in Table 2. At 573 K, decomposition does not occur: the precursor recrystallizes on the cold part of the reactor beyond the substrates. Moreover, decomposition occurs from 623 K to 873 K but no deposit is formed between 673 and 823 K. This indicates that the kinetics of formation of the deposit varies as a function of the substrate temperature. This feature was previously observed in the case of the study of Cp_2V as a precursor to vanadium carbide[30] and was explained by the deposition of a different type of coating, mainly oxide at low temperature in contrast to carbide at high temperature. SEM observation of the deposits shows a nodular surface at 623 K and a smoother one at 873 K. The film thickness, measured on cross-sections, was higher at 623 K than at 873 K (2.5 and 1.5 μm, respectively). EDS analyses indicated the presence of vanadium, carbon and oxygen

Table 2 Selected CVD conditions for Cp_2VMe_2 and corresponding analysis of the deposits

Mass of precursor (mg)	Pressure (Torr)	Nitrogen flow rate ($l\,h^{-1}$)	Substrate temperature (K)	Substrate type	Deposit composition from XPS[a] (at%)		
					V	C	O
700	5	7	623	Steel	38	20	42
1500	4	7	873	Steel	35	31	34
1500	2	3	873	Steel	35	31	34

[a] Semi-quantitative results.

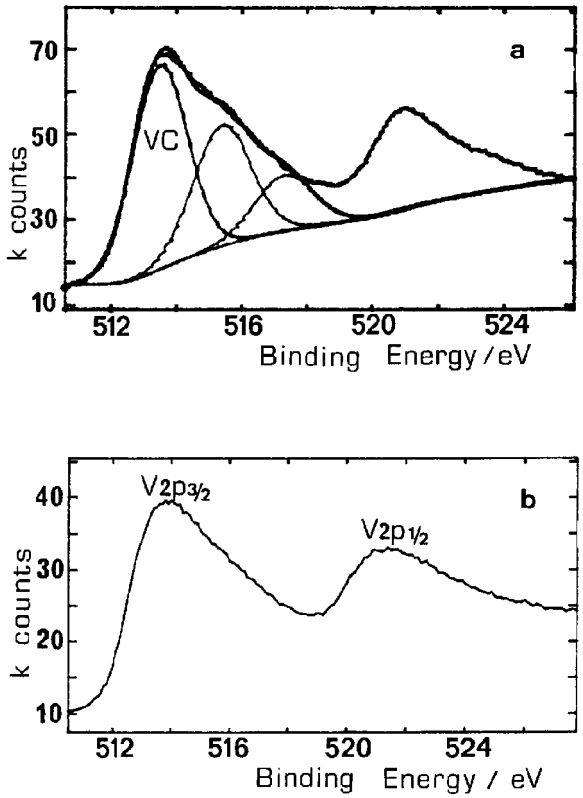

Figure 8 XPS analysis of the deposits obtained from Cp_2VMe_2 showing the presence of vanadium carbide (a) at 623 K and (b) at 873 K.

(cf. section 2.1) at 623 and 873 K. XPS analyses confirmed these results. The atomic compositions of the deposits are reported in Table 2. An increase in the amount of carbon was observed with increasing temperature. As a consequence, the V/C ratio at 873 K was half of that at 623 K. Brown and Maya[31] have studied Cp-containing vanadium carbide precursors and attributed the larger amounts of carbon obtained at 873 K to the dehydrogenation of the Cp groups that resulted, after the opening of the ring, in the formation of lower-molecular-mass species that reacted at the substrate surface. Moreover, the films did contain vanadium carbide, as proved by the XPS spectrum (513.4 eV component of the V $2p_{3/2}$ peak) shown in Fig. 8(a) for a substrate temperature of 623 K. The other two components of the V $2p_{3/2}$ signal at 515.4 and 517.4 eV correspond to vanadium oxycarbide and oxide.[32–34] At 823 K the XPS spectrum of the film shows similar features, confirming the presence of vanadium carbide at this temperature (Fig. 8b).

2.3 CVD using $CpTiCl_2N(SiMe_3)_2$ and Cp_2VMe_2 simultaneously

From the independent study of $CpTiCl_2N(SiMe_3)_2$ and Cp_2VMe_2 described above, the set of CVD conditions that may allow these precursors to co-decompose and form ceramics containing vanadium *and* titanium appeared to be the following: the substrate temperature should be set at either 623 or 873 K (but not in between), the pressure at 5 Torr, and the nitrogen flow rate at 7 l h^{-1}. Surprisingly, the initial experiments conducted using these conditions did not lead to the incorporation of vanadium in the films (Table 3, experiments 1, 4 and 7). In subsequent experiments under nitrogen and helium the pressure and gas flow rate had to be adjusted in order to solve this problem. Simultaneous decomposition of the precursors occurred

Table 3 Conditions of co-decomposition of $CpTiCl_2N(SiMe_3)_2$ and Cp_2VMe_2 and corresponding analysis of the deposits

Experiment no.	Carrier gas	Substrate type	Substrate temperature (K)	Mass of precursors (mg)		Pressure (Torr)	Carrier gas flow rate (1 h^{-1})		Deposit thickness (μm)	Deposit composition from XPS[b] (at%)				
				[Ti][a]	[V][a]		[Ti][a]	[V][a]		V	Ti	C	N	O
1	N_2	Si, steel	623	390	370	6	7	7		(Ti, C, O, no V)[c]				
2	N_2	Si	623	350	300	50	2.5	2.5	1	19	12	18	0	49
3	N_2	Steel	623	350	300	50	2.5	2.5	1	11	20	20	0	49
4	N_2	Si	873	390	370	5	7.5	7		(Ti, C, O, no V)[c]				
5	N_2	Si	873	300	300	50	3	2.5	1	18	7	48	5	20
6	He	Steel	623	130	120	7	2	2	<1	15	17	11	0	56
7	He	Si, steel	873	420	300	6	2.5	2.5		(Ti, C, O, no V)[c]				
8	He	Steel	873	320	230	8	2	2	1	11	16	15	3	54

[a] [Ti], $CpTiCl_2N(SiMe_3)_2$; [V], Cp_2VMe_2.
[b] Semi-quantitative results.
[c] EDS results.

under the conditions listed in Table 3, experiments 2, 3, 5, 6 and 8. From EDS and XPS analyses of these deposits formed on silicon and steel substrates, the following general observations may be noted.

(1) Titanium and vanadium are always present in the deposits.
(2) At 873 K and under nitrogen, an increase of the pressure up to 50 Torr is necessary to observe all four elements in the deposits (Table 3, experiment 5). However, at the same pressure but at a lower temperature of 623 K, nitrogen is missing (Table 3, experiments 2 and 3).
(3) At 873 K, incorporation of nitrogen is also observed under helium (Table 3, experiment 8). In this case, the nitrogen atoms of the deposit only originate from the titanium precursor. On the other hand, when the carrier gas is nitrogen, the presence of nitrogen in the films may also result from the dissociation of N_2 which conceivably could be catalyzed in the presence of transition-metal complexes.
(4) Chlorine is not detected in the films. Silicon does not appear systematically and its amount is always lower than 2%.
(5) The SEM observations of the deposits (Fig. 9) show a homogeneous and granular surface with larger grain sizes under helium than under nitrogen.
(6) XRD studies show that the deposits are only partially crystallized at both temperatures (Fig. 10). No accurate assignment of the few weak peaks observed could be made by comparison with known titanium and vanadium carbide, nitride or oxide phases.
(7) In all cases, the film thickness was estimated at approx. 1 μm.

2.4 Atmospheric-pressure experiments

The potential of $Cp_2TiCl_2N(SiMe_3)_2$ and Cp_2VMe_2 to undergo co-decomposition to TiVCN thin films was further checked by carrying out CVD experiments under helium at atmospheric pressure, at 623 and 873 K. In such conditions, a 15 l h^{-1} gas flow rate (7.5 l h^{-1} for each precursor) and higher vaporization temperatures (see Section 3.3) were necessary to drive both precursors through the reactor. EDS analysis of the deposits showed the presence of titanium, vanadium, carbon and oxygen (Table 4, experiments 2 and 4). XPS data confirmed the deposition of the three elements vanadium, titanium and carbon but showed that nitrogen was not present. Contamination of the deposits by silicon was observed at atmospheric pressure and for both substrate temperatures: 4% and 1% at 873 and 623 K, respectively. It may have resulted from an early fragmentation of the Me_3Si groups of the titanium precursor, which was vaporized at a higher temperature at atmospheric pressure than it was at low pressure.

2.5 Analyses of decomposition products

The decomposition products condensed in the liquid-nitrogen trap during the 'two-precursor' CVD experiments under helium, and at low and atmospheric pressure, were dissolved in toluene for GC and GC–MS analyses and in toluene-d_8 for NMR studies (Table 4). Me_3SiCl, $(Me_3Si)_2NH$, CpH and CpMe species could be identified by GC analyses through the addition of internal references. GC–MS studies confirmed these results and also showed the presence of $C_5H_4Me_2$. However, the Me_3SiCl and $(Me_3Si)_2NH$ components were not observed in this case. In addition, products such as Me_3SiOH and $(Me_3Si)_2O$ resulting from the hydrolysis of Me_3Si radicals were detected [base peaks $[Me_2SiOH]^+$ (m/z = 75) and $[Me_3SiOSiMe_2]^+$ (m/z = 147)]. This was also noted in the TG–MS analysis of $CpTiCl_2N(SiMe_3)_2$.[22] Proton NMR spectra showed the typical signals corresponding to protons on *Me*$_3$Si, *Me*Cp, and Cp. It should be noted that the volatile CVD products were identical to those detected by TG–MS studies of separate precursors. They also contained other compounds that could not be identified. From the comparison of the identified species with those analyzed after independent CVD from $CpTiCl_2N(SiMe_3)_2$ and from Cp_2VMe_2, it seems that the precursors do not interfere in the gas phase before undergoing film formation at the substrate surface. The nature of the volatile products does not seem to differ with CVD temperature and pressure conditions.

2.6 'Two-precursor' CVD using the unit equipped with a high-vacuum diffusion pump and NH_3 as reactive gas

At this point, it may be stated that (i) oxygen content in the deposits is so high that the films may be just titanium–vanadium oxycarbides, and (ii) that the nitrogen content is much too low for stating

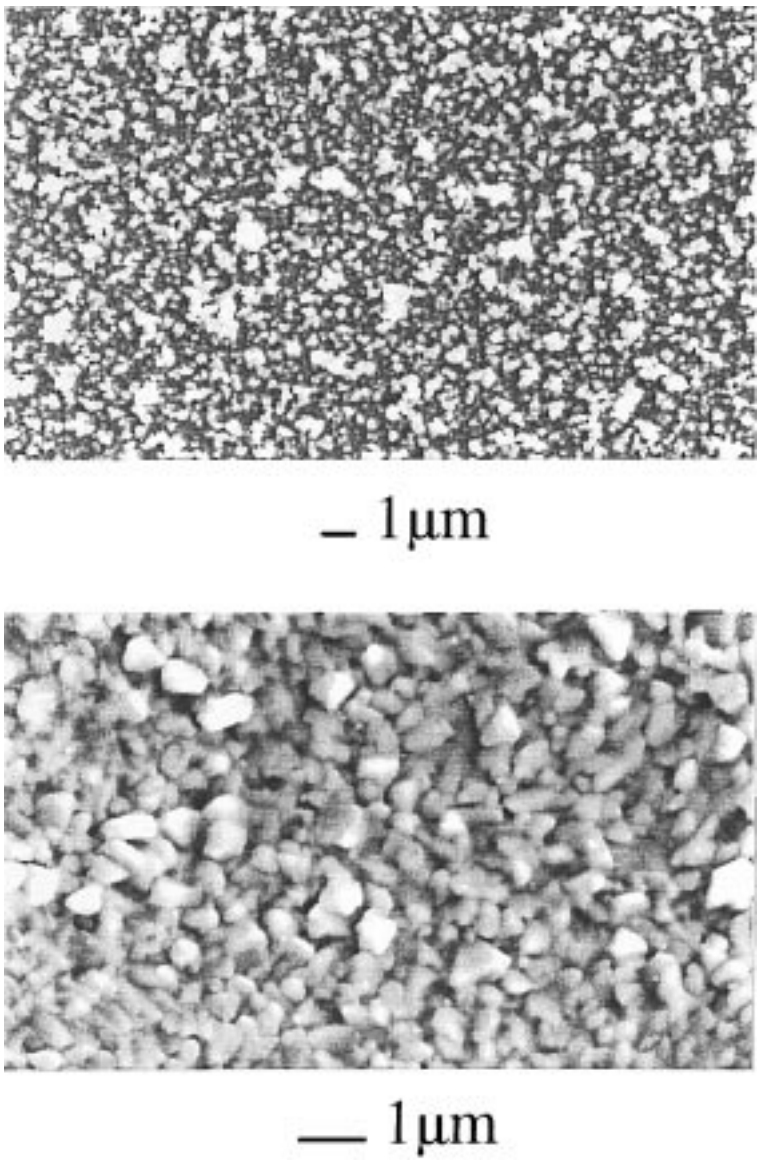

Figure 9 SEM of the deposits obtained from $CpTiCl_2N(SiMe_3)_2$ and Cp_2VMe_2. Substrate temperature: 873 K. N_2 (top) and He (bottom) carrier gas.

that titanium–vanadium carbonitride films have been obtained. Additional experiments using a CVD unit equipped with a high-vacuum diffusion pump and with helium as carrier gas showed that the oxygen content was considerably reduced from 40% down to less than 7% (Fig. 11). The nitrogen content was noticeably increased from 3% up to 12% when NH_3 was added to the reactive gas mixture (Table 5, experiments 2 and 3). Along with the decrease in the oxygen content down to 7%, the carbon contents of these films were correspondingly higher than those obtained by using the other CVD system equipped only with a primary pump. XPS analysis (Fig. 12) showed that the carbon was present as both carbide (10%) and graphite (46%). The addition of hydrogen to the reactive gas mixture might be effective in reducing the graphite content. It should be pointed out that the deposits then contained equal amounts of titanium, vanadium, carbon as carbide and nitrogen, i.e. approx.

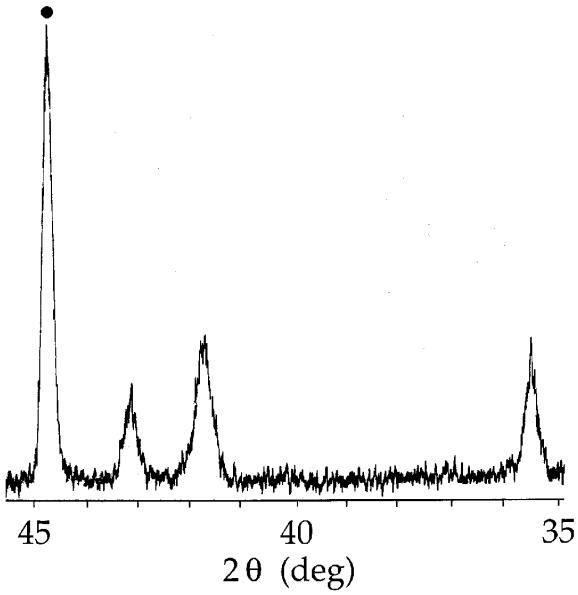

Figure 10 XRD pattern (main lines) of a deposit obtained from the co-decomposition of $CpTiCl_2N(SiMe_3)_2$ and Cp_2VMe_2. ● Line due to the substrate.

10%. As shown on Fig. 13 homogeneous deposits 1 μm thick were obtained. XRD studies showed that they were not crystallized.

3 EXPERIMENTAL

3.1 General procedures

All manipulations were carried out by using standard Schlenk and dry-box techniques under argon. Solvents were dried and distilled over sodium benzophenone ketyl. $CpTiCl_2N(SiMe_3)_2$ and Cp_2VMe_2 were prepared via previously reported methods.[22–25] $CpTiCl_2N(SiMe_3)_2$ was purified by recrystallization from hexane[22] and Cp_2VMe_2 was sublimed. After purification, the compounds were stored in sealed ampules under argon.

3.2 Analytical techniques

Gas chromatography (GC) data were recorded on a Intersmat GC-121-DFL chromatograph (10% SE30/Chromosorb/DAW 80/100/1.5 m column) and GC–MS data on a DELSI DI 200 chromatograph (capillary Supelco/30 m column) coupled to a Nermag Model R10-10H EI mass spectrometer. Standard mass spectrometry (MS) analyses were conducted directly on the same spectrometer. ^{1}H NMR were recorded in toluene-d_8 on a Bruker WM 200 or WM 250 spectrometer. Scanning electron microscopy (SEM) observations of the deposits were performed on a JEOL JMS 840A unit

Table 4 CVD under helium from $CpTiCl_2N(SiMe_3)_2$ and Cp_2VMe_2 at atmospheric and low pressure: analysis of the deposits by EDS and XPS and of the exhaust gases by GC, GC–MS and ^{1}H NMR

Experiment no.	CVD conditions: Temperature (K)	CVD conditions: Pressure (Torr)	EDS: Atoms found	XPS: Atoms found	GC: Detected species	^{1}H NMR in toluene-d_8 (δ ppm)	GC–MS: Detected species (m/z)
1	623	9	Ti	Ti	CpH	*Me*$_3$Si	CpH (66)
			V	V	CpMe	*Me*Cp (2.12)	$[Me_2SiOH]^+$ (75)
			C	C	Me_3SiCl		CpMe (80)
			O	O	$HN(SiMe_3)_2$		$C_5H_4Me_2$ (94)
							$[Me_3SiOSiMe_2]^+$ (147)
2	623	P_{atm}	Ti	Ti	CpH	—	CpH (66)
			V	V	CpMe		$[Me_2SiOH]^+$ (75)
			C	C	Me_3SiCl		CpMe (80)
			Si	Si			$C_5H_4Me_2$ (94)
			Cl				$[Me_3SiOSiMe_2]^+$ (147)
			O	O			
3	873	9	Ti	Ti	CpH	*Me*$_3$Si	CpH (66)
			V	V	CpMe	CpH (6.05)	$[Me_2SiOH]^+$ (75)
			C	C	Me_3SiCl		CpMe (80)
				N			$[Me_3SiOSiMe_2]^+$ (147)
			O	O			
4	873	P_{atm}	Ti	Ti	CpH	*Me*$_3$Si	CpH (66)
			V	V	CpMe	*Me*Cp (2.12)	$[Me_3SiOSiMe_2]^+$ (147)
			C	C	Me_3SiCl		
			Si	Si			
			O	O			

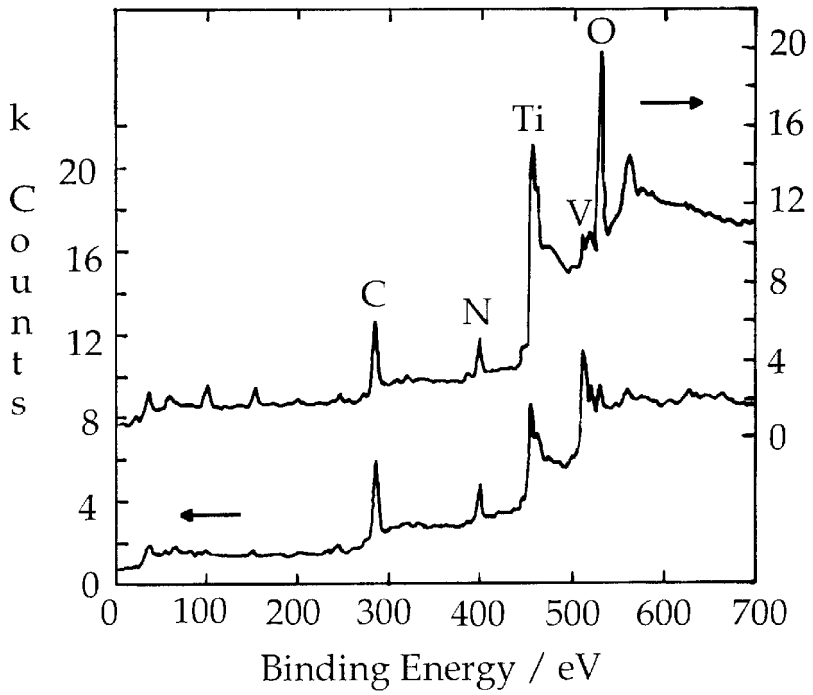

Figure 11 XPS of the deposits obtained from the co-decomposition of $CpTiCl_2N(SiMe_3)_2$ and Cp_2VMe_2. Primary pumping conditions (upper trace), after purification of the CVD apparatus with a secondary pumping system (lower trace).

equipped with an energy-dispersive spectrometry (EDS) analyser. The voltage acceleration was kept constant (15 kV) in all analyses. Elemental analysis of the deposits was determined by X-ray photoelectron spectroscopy (XPS) using a VG Escalab Model MK2 (MgKα radiation, 1253.3 eV) after sputtering the surface with an Ar^+ ion beam. Semi-quantitative results were obtained using standards and sensitivity factors taken from Scofield tables.[35] Electron microprobe analyses (EPMA) were performed on a Cameca SX-50 apparatus equipped with three wavelength-dispersive spectrometers (WDS). Thermal analyses including thermogravimetry (TG) and differential thermal analysis (DTA) were carried out using a Setaram TG-DTA 92 system coupled to a Leybold–Heraeus QX 2000 quadrupolar mass spectrometer (QMS) through a capillary that let the gas phase continuously enter the analysis chamber. Thermal studies were performed in dynamic mode and in isothermal mode by following previously reported procedures.[36]

Table 5 Conditions of co-decomposition of $CpTiCl_2N(SiMe_3)_2$ and Cp_2VMe_2 in high-purity CVD equipment and corresponding analysis of the deposits.

Experiment no.	Carrier gas	Reactive gas	Substrate temperature (K)	Mass of precursors (mg)		Pressure (Torr)	Carrier gas flow rate (1 h^{-1})		Reactive gas flow rate (1 h^{-1})	Deposit composition from XPS[b] (at%)				
				[Ti][a]	[V][a]		[Ti][a]	[V][a]		V	Ti	C	N	O
1	He	—	873	545	330	10	2	2	—	(No O detected)[c]				
2	He	NH_3	873	700	420	10	2	2	3	10	10	56	12	7
3	He	NH_3	873	660	350	15	3	3	3	10	10	56	12	7

[a] [Ti], $CpTiCl_2N(SiMe_3)_2$; [V], Cp_2VMe_2.
[b] Semi-quantitative results.
[c] EDS results.

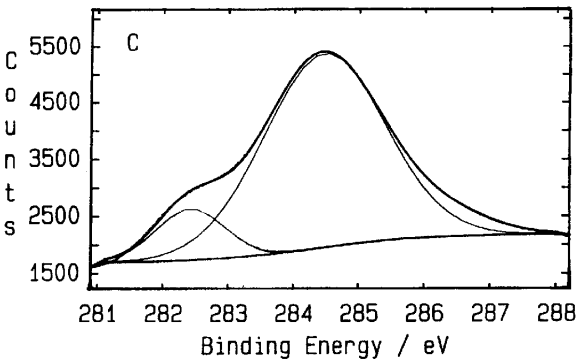

Figure 12 XPS analysis (carbon region) of a deposit obtained from $CpTiCl_2N(SiMe_3)_2$ and Cp_2VMe_2. Substrate temperature: 873 K. He carrier gas, NH_3 reactive gas.

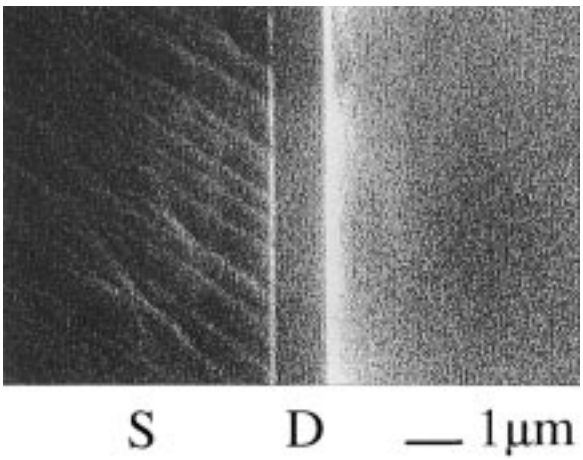

Figure 13 SEM of the cross-section of a deposit obtained from $CpTiCl_2N(SiMe_3)_2$ and Cp_2VMe_2. Substrate temperature: 873 K. He carrier gas, NH_3 reactive gas. S, substrate; D, deposit.

3.3 Chemical vapor deposition (CVD)

The deposition of thin films was carried out in three hot-wall CVD units differing by the precursor driving system or the pumping unit.

The first unit has been previously described[36] and was used for the independent CVD study of $CpTiCl_2N(SiMe_3)_2$ and Cp_2VMe_2. The second unit, used for the two-precursor experiments, differed from the former by the precursor-driving systems which consisted of two identical linear-type saturators heated with heating tapes wrapped around the tube (Fig. 14). The temperatures of the precursors were measured with K-type thermocouples. In both sets of equipment, ASM mass flow meters were used to control the gas flow rates. The precursors were heated at their vaporization temperatures, determined by preliminary TG and DTA analyses (*vide infra*) (Cp_2 VMe_2, 80 °C/low pressure, 100 °C/atmospheric pressure; $CpTiCl_2N(SiMe_3)_2$, 125 °C/low pressure, 150 °C/atmospheric pressure). These first two sets of equipment were connected to a high-flow-rate (12 m^3 h^{-1}) primary pump (Edwards E2M12). The poor efficiency of this pumping system in purging the CVD reactor before the experiment led us to use another unit.

This third unit was equipped with U-type saturators and a high-vacuum (10^{-6} Torr) diffusion pump. Electronic-grade helium was used as carrier gas. Before the experiment was started, the reactor and the lines between the saturators and the reactor were heated at 423 K and 373 K, respectively, for 12 h at 10^{-6} Torr. NH_3 was added to the gas flow between the saturator and the reactor.

The saturators were loaded inside an argon-filled dry box in order to prevent, as much as possible,

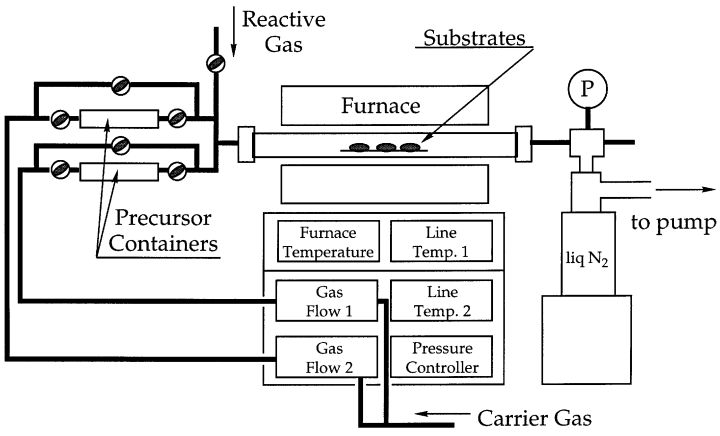

Figure 14 Hot-wall CVD apparatus.

oxygen and water contamination. Si(100) and 35CD4 steel substrates were located in the constant-temperature zone of the furnace of the units. They were pretreated as follows: Silicon substrates were cleaned in H_2SO_4/H_2O_2 (1:4), rinsed in distilled water and dried; steel substrates were mechanically polished using abrasive paper (grade 600–4000) and diamond paste, and sonicated in an ethanol bath.

The film thickness was estimated either by measuring the cross-section (silicon substrate) or by comparing the film (Ti, V)/steel substrate (Fe) EDS signals. In most cases, the thickness was approx. 1 μm.

As (i) the deposits were very thin, (ii) the precursor mass was not constant (350–1500 mg), (iii) deposition occurred in such hot-wall reactors on both the substrate and the reactor walls, and although the duration of all experiments was kept constant at 3 h, the actual deposition time could not be determined, nor the deposition rate.

Acknowledgments This work, carried out within collaborative CNRS–PIRMAT ARC and CPR programs, was supported by the CNRS and Ascometal company (Ph.D. grant to C.D.), the French Research and Education Ministry (Ph.D. grant to B.C.), the DGA-DRET (Groupe 8) of the French National Defense Ministry, Aérospatiale and Giat Industries companies, and the Conseil Régional Midi-Pyrénées. We thank C. Claparols and S. Richelme for MS analysis, L. Noé for GC–MS studies, G. Chatainier and E. Provincial for XPS data on separate precursors, and D. Oquab for SEM–EDS studies. Special thanks go to F. Maury and S. Abisset for the use of their high-purity CVD unit and to R. Berjoan and F. Sibieude for XPS and XRD analyses of the quaternary deposits.

REFERENCES

1. Y. Deguilhem, *CNRS* **41**, 13 (1993).
2. M. J. Hampden-Smith, W. G. Klemperer and C. J. Brinker (eds), *Better Ceramics through Chemistry V, MRS Symp. Proc.* **271** (1992).
3. *Proc. IX Europ. Conf. on CVD, J. Phys.* Suppl. 8, 1993.
4. G. W. Cullen and K. E. Spears (eds), *Proc. XI Int. Conf. on CVD*, 1990 The Electrochemical Society, Pennington, NJ, USA.
5. R. M. Laine, B. J. Aylett, J. Livage, D. Schleich and R. J. P. Corriu, in: *Transformation of Organometallic Compounds into Common and Exotic Materials: Design and Activation*, Laine R. M. (ed), NATO ASI Ser., Martinus Nijhoff, Dordrecht, The Netherlands 1986, p. 241.
6. L. Valade, R. Choukroun, P. Cassoux, F. Teyssandier, L. Poirier, M. Ducarroir, R. Feurer, P. Bonnefond and F. Maury, in: *The Chemistry of Transition Metal Carbides and Nitrides*, Oyama, S. T. (ed), Blackie Academic and Professional, Glasgow 1996, pp. 290–310, and references cited therein.
7. L. Poirier, O. Richard, M. Ducarroir, F. Teyssandier, F. Laurent, O. Cyr-Athis, R. Choukroun, L. Valade and P. Cassoux, *Thin Solid Films* **249**, 62 (1994).
8. Y. Derraz, O. Cyr-Athis, R. Choukroun, L. Valade, P. Cassoux, F. Dahan and F. Teyssandier, *J. Mater. Chem.* **5**, 1775 (1995).
9. P. Bonnefond, R. Feurer, A. Reynes, F. Maury, B. Chansou, R. Choukroun and P. Cassoux, *J. Mater. Chem.* **6**, 1501 (1996).
10. F. Laurent, Ph. Michel, R. Feurer, R. Morancho, L. Valade, R. Choukroun and P. Cassoux, *J. Mater. Chem.* **3**, 659 (1993).
11. R. M. Fix, R. G. Gordon and D. M. Hoffman, *Chem. Mater.* **2**, 235 (1990).
12. R. M. Fix, R. G. Gordon and D. M. Hoffman, *Chem. Mater.* **3**, 1138 (1991).
13. C. H. Winter, J. W. Proscia, A. L. Rheingold and T. S. Lewkebandara, *J. Inorg. Chem.* **33**, 1227 (1994).
14. L. E. Toth, *Transition Metal Carbides and Nitrides, Refractory Materials*, Margrave, J. L.(ed), Academic Press, New York, 1971.
15. R. Juza, in: *Advances in Inorganic Chemistry and Radiochemistry*, Vol. 9, Emeleus, H.J. and Sharpe, A.G. (eds), Academic Press, New York, 1966, pp. 81–131.
16. I. I. Bilyk, *Poroshkovaya Metallurgiya* **114**, 49 (1972).
17. A. A. Adomovskii, A. I. Bezykornov and I. I. Bilyk, *Poroshkovaya Metallurgiya* **136**, 79 (1974).
18. L. Ramqvist, *Jernkont. Ann.* **152**, 465 (1968).
19. M. C. Schouler, M. Ducarroir and C. Bernard, *Rev. Iter. Hautes Temp. Refract. Fr.* **20**, 261 (1983).
20. D. M. Hoffman, *Polyhedron* **13**, 1111 (1994).
21. G. S. Girolami, J. A. Jensen, D. M. Pollina, W. S. Williams, A. E. Kaloyeros and C. M. Alloca, *J. Am. Chem. Soc.* **109**, 1579 (1987).
22. F. Laurent, J. S. Zhao, L. Valade, R. Choukroun and P. Cassoux, *J. Anal. Appl. Pyrol.* **24**, 39 (1992).
23. C. Airoldi, D. C. Bradley, H. Chudzynska, M. B. Hursthouse, K. M. Abdul Malik and P. R. Raithby, *J. Chem. Soc., Dalton Trans.* 2010 (1980).
24. Y. Bai, H. W. Roesky and M. Notelmeyer, *Z. Anorg. Allgem: Chem.* **595**, 21 (1991).
25. E. Samuel, D. F. Foust and M. D. Rausch, *J. Organometal. Chem.* **193**, 209 (1980).
26. S. B. Kim, S. K. Choi, S. S. Chun and K. H. Kim, *J. Vac. Sci. Technol: A: Vac.* **9**, 2174 (1991).
27. *Eight-Peak Index of Mass Spectrometry*, Mass Spectrometry Data Center, Chemical Society, London 1974, Vol. 3, Part 1.
28. G. J. Erskine, D. A. Wilson and J. D. McCowan, *J. Organometal. Chem.* **114**, 119 (1976).
29. H. G. Alt, F. P. di Sanzo, M. D. Rausch and P. C. Uden, *J. Organometal. Chem.* **107**, 257 (1976).
30. L. Poirier, O. Richard, M. Ducarroir, F. Teyssandier, F. Laurent, O. Cyr-Athis, R. Choukroun, L. Valade and P. Cassoux, *Thin Solid Films* **249**, 62 (1994).
31. G. M. Brown and L. Maya, *Inorg. Chem.* **28**, 2007 (1989).

32. A. N. MacInnes and A. R. Barron, *Polyhedron* **13**, 1315 (1994).
33. P. Mériaudeau and J. C. Vedrine, *Nouv. J. Chim.* **2**, 133 (1978).
34. C. Blaauw, F. Leenhouts, F. van der Woode and G. A. Sawatzky, *J. Phys.* **C8**, 459 (1976).
35. J. H. Scofield, *J. Electron. Spectroc. Rel. Phenom.* **8**, 129 (1976).
36. B. Chansou, R. Choukroun and L. Valade, *Appl. Organometal. Chem.* **11**, 195 (1997).

